Performance measurement of capture mask, including characterisation of full operating performance

Prepared for
The PROTECT COVID-19 National Core Study on transmission and environment

PROTECT (2023)
National Core Study Report

Prepared 2023
First published 2023

The PROTECT COVID-19 National Core Study on transmission and environment is a UK-wide research programme improving our understanding of how SARS-CoV-2 (the virus that causes COVID-19) is transmitted from person to person, and how this varies in different settings and environments. This improved understanding is enabling more effective measures to reduce transmission – saving lives and getting society back towards 'normal'.

This report details experimental studies designed to investigate the performance of a new facemask design with impactor plate capabilities for segregating aerosols and droplets by size. This includes collecting and analysing the particle size distributions, temperature and relative humidity monitoring in each section of the face mask using human subjects. Key findings from the study are: the mask effectively segregates the particle size in some subjects; there is a significant 'natural variability' between human subjects in particle size distributions in time and space, and; facemask measurements demonstrate distinct differences between mouth and nose breathing.

This report and the research it describes were funded by the PROTECT COVID-19 National Core Study on transmission and environment, which is managed by the Health and Safety Executive (HSE) on behalf of HM Government. Its contents, including any opinions and/or conclusions expressed, are those of the authors alone and do not necessarily reflect UK Government or HSE policy.

Performance measurement of capture mask, including characterisation of full operating performance

Dr Waseem Hiwar[1], Dr Gareth Keevil[2], Dr James McQuaid[2], Prof Nikil Kapur[3], Prof David Hodgson[2], Dr Peter Culmer[2], Prof Catherine Noakes[1]

[1] School of Civil Engineering, University of Leeds, LS2 9JZ, UK
[2] School of Earth and Environment, University of Leeds, LS2 9JZ, UK
[3] School of Mechanical Engineering, University of Leeds, LS2 9JZ, UK

Executive Summary

The Covid-19 pandemic has demonstrated the need for rapid understanding of how a new disease spreads. It is crucial that rapid and appropriate public health interventions and environmental health measures are developed. The pandemic has vividly highlighted that better informed and earlier interventions can minimise transmissions, and limit socio-economic impacts. One crucial piece of evidence that have proven very challenging to quantify and understand, and therefore model, is the role of exhaled aerosols in spreading disease.

Aerosols in human exhalations range from 0.1-to over 100 µm (e.g., Milton 2020; Wang et al., 2021), and pathogen-containing aerosol size controls transmission routes. Larger aerosols, which quickly settle onto surfaces, require close contact or surface transmission, while smaller aerosols can remain suspended for hours. Existing instrumentation to size-segregate exhaled aerosols is impractical for large-scale studies, due to size, expense, and availability. There was a clear need to develop best practice for mask wearing and design robust healthcare equipment protocols.

As part of the HSE-funded PROTECT Covid-19 National Core Study, we have developed novel experiments in the Sorby Laboratory. The performance measurements demonstrate the potential to engineer a new type of facemask that separates aerosols into size fractions using physical simulations and human subjects.

This report summarises the work relating to Theme 2 activity: validated Leeds Face Masks. This study conducted laboratory experiments to evaluate the performance of a facemask capable of segregating the particle size of exhaled human breath. The study considers the parameters of temperature and relative humidity within the three mask regions.

Key findings from the study are:

- The mask effectively segregates the particle size in some subjects
- There is a significant 'natural variability' between human subjects in particle size distributions in time and space.
- Facemask measurements demonstrate distinct differences between mouth and nose breathing.

This research shows that the potential for size segregation within a mask remains a viable approach. However, the process interactions and environmental controls are complicated, and that the design and validation of facemasks capable of reliable and reproducible size-segregation remains an ongoing challenge, but with the tantalising potential to revolutionise the monitoring of infectious airborne viruses.

Introduction

Facemasks are commonly used to protect a wearer and others from airborne droplets and particulates. Whilst at one time this was only routine in hospitals, the recent Covid-19 crisis has seen widespread use of masks by the general public. There is a wide range of masks available, from homemade masks to officially tested and regulated masks. Masks can also contain elements to sample the wearer's breath, as demonstrated in a previous study using strips as an accurate and non-invasive method of diagnosing tuberculosis (Williams, et al., 2014; 2020). A novel facemask was developed in the first stage of Theme 2 activity (see Methodology below). Here, we report the initial experiments and analysis for the validation of the facemask's capacity to segregate droplet sizes through human studies, which can contribute to understanding of the disease transmission mechanisms. By examining fluid dynamics in facemasks, we can improve our knowledge of air circulation and changing environmental conditions during breathing.

This report details experimental studies designed to investigate the performance of the new facemask design with impactor plate capabilities for segregating aerosols and droplets by size. This includes collecting and analysing the particle size distributions, water-sensitive paper, temperature and relative humidity monitoring in each section of the face mask (near face, middle chamber, and far chamber).

Human exhalations study

Methodology

The human exhalation study was conducted in a specialist laboratory with a positive pressure to reduce the impact of external particles. The facemask used was based on an original Mayku mask body. New components added include vacuum formed components from 3D printed moulds consisting of a funnel with 8 mm diameter nozzle, a cylinder component, a reduced version of the original cap, and an impactor plate made of the same vacuum formed material glued by hand part way along the cylinder (**Figure 1**). The original Mayku mask was vacuum formed using a Mayku machine from 3D printed components. Creating the second prototype components in the same way, and designing them to interact with this original design, leads to a highly customisable and lightweight mask already demonstrated to have acceptable face fit. Additionally, using separate components for the nozzle, cylinder containing the impactor plate, and the cap allows sampling on any surface within the mask. Initial testing of both prototypes using water sensitive paper and the GRIMM optical particle counter indicates that moisture reaches the cap, though in reduced levels compared with that reaching the impactor plate (March 2022 PROTECT report).

The multizone facemask with regions separated by impactor stages was utilised and linked to a GRIMM optical particle counter model 1.108 via a small tube embedded within the mask (**Figure 1**). THe GRIMM optical particle counter measures particles ranging in size from 0.3 µm to 20 µm, with readings every 6 seconds (Grinshpun, et al., 2016). A custom in-house designed data logger was used to measure the temperature and relative humidity (sensor: HIH8121-021-001).

Ten (10) participants were recruited for the study (50: 50, male: female), and each participant signed an ethics approved statement. Four of the participants (two females and two males) breathed through the mouth only for one experimental run, and then through the nose only for a second run. The remaining six participants performed a single experiment with combined mouth and nose breathing.

Each facemask was washed with warm soapy water, dried thoroughly, and then wiped with an alcohol solution (70% isopropyl alcohol) prior to each test subject.

Each participant wore the facemask and breathed for two minutes through the nose only, the mouth only, or a combination of mouth and nose breathing for each region of the mask (1: Near face, 2: Middle chamber, and 3: Far chamber) separately (**Figure 1**). Before each breathing test, the background conditions inside the chamber were measured to determine the level of background aerosols on the results.

Water-sensitive paper strips (from Syngenta) were adhered inside the near face and middle chambers to provide an immediate and obvious indication of the location of exhaled droplets or condensed water from gas phase. The paper changes from yellow to dark blue in the presence of water, providing a rapid and highly visual indication of exhaled droplet locations. Strategically positioned, these can be used to identify suitable locations for diagnostic strips. Additionally, the paper can be used for rough droplet sizing. According to Q.Instruments [2008], the paper strips can be used to size droplets of 60 µm.

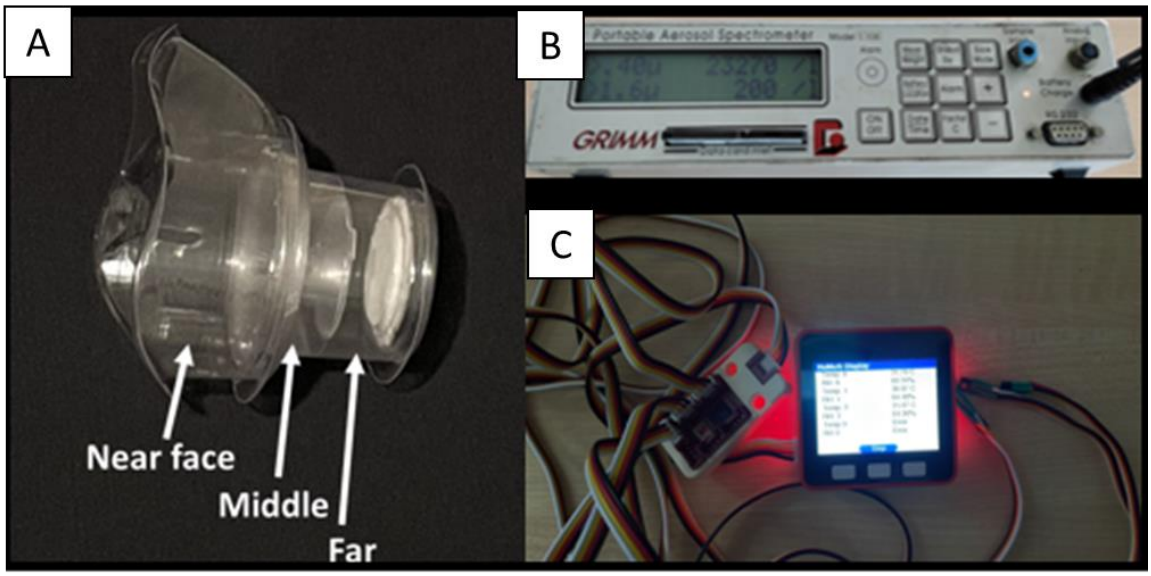

Figure 1: A) A multizone facemask, B) a GRIMM optical particle counter model 1.108, and C) a temperature and relative humidity sensor data logger.

Results

Particle size segregation

Table 1 records the statistical information for each participant, including the mean and standard deviation (minimum and maximum) for particle size, temperature, and relative humidity, in the near, middle, and far chamber. **Figure 2 (A)** shows the particle count of exhaled aerosols and droplets as a function of time for particle sizes of 0.3/ 0.4/ 0.5/ 0.65/ 0.8/ 1.0/ 1.6/ 2/ 3/ 4/ 5/ 7.5/10/15/20 µm. The 5-20 µm range are grouped due to the lower number of counts. After one minute of breathing, most small particle sizes exhibit a distinct fluctuation indicating inhalation (reduction in particle number) and exhalation (increase in particle number) in the near face and middle chamber. For the same participant, facemask temperature reaches a steady state after one minute, while the relative humidity steady state is reached in less than 20 seconds **(Fig. 2B)**. For participants one and six (**Figure 3 A**), and participant four and seven mouth breathing, it is evident that the facemask was able to effectively separate particles of sizes 5-20 µm, as these particles were observed in the chambers near the face and in the middle, while are absent in the far section (green cells in **Table 1**). In all other participants for combined, mouth or nose only trace (2 or less particle measurements) were recorded in the 5-20 µm range in the far chamber (blue cells in **Table 1**) (**Figure 3 B**), and only participant 5 (mouth) had more than 2 counts in the far chamber for the 5-20 µm range.

Table 1: Summary of particulates of varying size, temperature, and relative humidity in each zone of a chamber for each participant. The green cells denote complete removal of larger sizes (5-20 µm), and blue cells denote trace (2 or less counts) of larger sizes (5-20 µm) in the far chamber.

Participant	Sampling point	Breathing type	Particle count Particle size (Mean ± SD [Min-Max])												
			0.3µm	0.4µm	0.5µm	0.65µm	0.8µm	1µm	1.6µm	2µm	3µm	4µm	5-20µm	Temp	RH
1	Near face	Combine	472.5 ± 82.1 (315-585)	272.5 ± 92.3 (165-485)	113 ± 38.4 (55-180)	42.5 ± 18.0 (15-70)	14.5 ± 8 (0-25)	8.5 ± 7 (0-20)	3.8 ± 4.3 (0-15)	2.5 ± 1.9 (0-12)	1.5 ± 1.8 (0-5)	0.5 ± 1.2 (0-5)	0.1 ± 0.5 (0-3)	23.9 ± 1.3 (21.7-26.7)	93.1 ± 3.9 (79.5-100)
	Middle		240.5 ± 59.1 (125-310)	100.5 ± 29.1 (45-155)	51 ± 18.5 (15-80)	17.8 ± 9.4 (5-35)	9.3 ± 6.8 (0-25)	6 ± 5.8 (0-20)	3.8 ± 3.9 (0-15)	1.8 ± 2.1 (0-9)	1.5 ± 2.2 (0-8)	0.6 ± 1 (0-3)	0.0 ± 0.0 (0-0)	22.1 ± 0.7 (20.8-22.8)	99.7 ± 0.6 (97.8-100)
	Far		218.8 ± 62.3 (90-325)	93.8 ± 34.4 (20-155)	39.3 ± 16.6 (5-80)	17.3 ± 11.9 (0-50)	12.5 ± 10.9 (0-40)	7.5 ± 8.5 (0-30)	6.5 ± 7.6 (0-25)	3.4 ± 3.7 (0-15)	3.2 ± 3.6 (0-14)	0.4 ± 0.8 (0-3)	0.0 ± 0.0 (0-0)	21.5 ± 0.7 (19.9-22.5)	99.9 ± 0.3 (98.7-100)
2	Near face	Combine	586.6 ± 166.3 (385-856)	299.3 ± 111.1 (170-485)	165.3 ± 81.1 (55-295)	73.5 ± 51 (15-170)	42.5 ± 38.3 (0-125)	33.3 ± 32.1 (0-110)	21.3 ± 23.8 (0-85)	9.6 ± 7.8 (0-25)	8.6 ± 7.6 (0-20)	1.3 ± 1.3 (0-4)	0.01 ± 0.1 (0-1)	25.8 ± 0.9 (23.9-27.7)	92.1 ± 3.4 (85.2-99.4)
	Middle		515.6 ± 86.8 (385-706)	267.6 ± 56.5 (175-375)	161.1 ± 48.2 (70-245)	76.3 ± 30.8 (25-125)	52.4 ± 25.9 (15-95)	41.6 ± 21.2 (15-75)	28.1 ± 18.3 (5-65)	17.3 ± 7.9 (5-38)	16.3 ± 7.5 (5-28)	2.4 ± 1.8 (0-7)	0.06 ± 0.24 (0-1)	23.9 ± 0.8 (22.2-24.8)	96.5 ± 3.2 (89.9-100)
	Far		339.7 ± 110.3 (205-625)	170.5 ± 57.6 (90-300)	92.1 ± 32.7 (50-165)	43.4 ± 22.3 (15-90)	28.7 ± 18.4 (5-70)	22.4 ± 15.7 (5-50)	13.4 ± 12.7 (0-45)	6.9 ± 5.4 (0-23)	4.9 ± 5.7 (0-17)	0.9 ± 1.2 (0-5)	0.02 ± 0.14 (0-1)	23.3 ± 1.1 (21-24.6)	97.9 ± 2.6 (92.9-100)
3	Near face	Mouth	607.1 ± 90.3 (455-761)	295.8 ± 61.3 (205-380)	145.5 ± 40.5 (85-220)	59.5 ± 24.9 (15-110)	31.8 ± 18.9 (4-61)	22.3 ± 15.3 (0-50)	13.3 ± 10.7 (0-35)	9.3 ± 3.2 (0-15)	7.3 ± 3.9 (0-13)	0.6 ± 0.8 (0-2)	0.01 ± 0.09 (0-1)	26.1 ± 0.8 (25.1-26.9)	93.1 ± 6.9 (83.5-100)
	Middle		665.5 ± 81.3 (15-130)	142.4 ± 43.4 (5-85)	34.8 ± 20.2 (5-70)	25 ± 16.3 (0-60)	14.2 ± 7.3 (0-26)	14.0 ± 7.1 (0-28)	2.0 ± 1.4 (0-5)	0.2 ± 0.4 (0-1)	0.0 ± 0.3 (0-1)	0.0 ± 0.2 (0-1)	0.0 ± 0.0 (0-0)	22.9 ± 0.4 (21-23.3)	86.9 ± 6.4 (75.3-97.9)
	Far		470.3 ± 47.6 (375-621)	233 ± 42.13 (165-335)	133.5 ± 37.7 (65-225)	76.5 ± 30.95 (20-140)	57 ± 30.1 (5-120)	46.3 ± 24.9 (5-85)	36 ± 21.1 (0-70)	20.6 ± 10.4 (0-39)	17.6 ± 10.1 (0-29)	3.4 ± 1.2 (0-5)	0.14 ± 0.38 (0-2)	23.5 ± 0.7 (22-25.9)	97.7 ± 2.1 (92.7-100)
	Near face	Nose	635.4 ± 189.8 (265-891)	315.9 ± 104.5 (100-460)	173.7 ± 69.4 (50-290)	81.3 ± 41.6 (10-160)	52.5 ± 33.8 (0-110)	42.9 ± 29.7 (0-95)	30 ± 22.1 (0-80)	16.2 ± 12.9 (0-44)	14.2 ± 12.2 (0-34)	2.4 ± 2.7 (0-12)	0.1 ± 0.3 (0-2)	24.9 ± 1.2 (22.5-25.4)	99.7 ± 1.3 (95.9-100)
	Middle		496.4 ± 100 (315-696)	223.8 ± 60.41 (140-360)	115.8 ± 46.55 (70-225)	46.8 ± 29.4 (0-105)	31.3 ± 24.1 (0-80)	23.3 ± 21.2 (0-80)	16.8 ± 17.6 (0-50)	12.2 ± 8.4 (0-36)	10.2 ± 8.9 (0-26)	1.8 ± 1.7 (0-6)	0.03 ± 0.17 (0-1)	23.4 ± 0.5 (23.3-24.9)	92.1 ± 5.5 (79.9-100)
	Far		510.9 ± 90.8 (365-676)	234.8 ± 65.6 (115-325)	122.3 ± 41.7 (50-200)	58.5 ± 28.2 (15-115)	43.6 ± 23.6 (10-85)	36.1 ± 23.9 (5-80)	27.0 ± 19.6 (5-65)	12.9 ± 6.7 (5-28)	12.7 ± 6.8 (5-25)	1.9 ± 1.5 (0-5)	0.06 ± 0.28 (0-2)	21.4 ± 0.7 (20-22.7)	97.2 ± 2.4 (91.2-100)
4	Near face	Mouth	342.5 ± 55.8 (240-465)	141 ± 42.5 (50-210)	62.8 ± 26.0 (20-110)	17.3 ± 12.7 (0-50)	6.5 ± 7.1 (0-30)	3.5 ± 5.6 (0-25)	0.7 ± 1.8 (0-5)	0.5 ± 1.4 (0-5)	0.4 ± 1.3 (0-5)	0.2 ± 0.5 (0-2)	0.0 ± 0.0 (0-0)	26.5 ± 0.8 (25.3-27.9)	93.3 ± 6 (77.9-100)

	Middle		402.8 ± 83.5 (265-555)	188.5 ± 70.8 (70-335)	98 ± 46.8 (30-195)	39.5 ± 26.4 (0-50)	19.3 ± 14.4 (0-50)	14.5 ± 11.1 (0-45)	8.5 ± 9.2 (0-35)	4 ± 3.6 (0-15)	3.8 ± 3.4 (0-13)	0.5 ± 1 (0-3)	0.06 ± 0.27 (0-2)	27.8 ± 0.5 (27-28.5)	81.1 ± 6.8 (71.8-92.8)
	Far		359.2 ± 122.7 (190-691)	166.9 ± 75 (60-400)	89.6 ± 55.3 (10-245)	32.2 ± 21.6 (0-85)	16.9 ± 15.2 (0-45)	13 ± 11.8 (0-35)	8.5 ± 9.8 (0-30)	4.4 ± 4.8 (0-20)	4 ± 4.9 (0-18)	0.4 ± 1.1 (0-5)	0.0 ± 0.0 (0-0)	26.7 ± 0.3 (26.2-27.2)	88.1 ± 6.4 (76.8-99.8)
	Near face	Nose	430.7 ± 164.6 (245-961)	183.3 ± 85.8 (70-405)	92.4 ± 63.4 (15-270)	33.5 ± 28.2 (0-0)	16.9 ± 17 (0-70)	12.8 ± 13.0 (0-55)	6.3 ± 7.7 (0-30)	3.1 ± 4.9 (0-22)	2.1 ± 3.7 (0-12)	0.7 ± 1.5 (0-7)	0.04 ± 0.21 (0-1)	26.2 ± 0.9 (24.2-27.7)	94 ± 6 (80.5-100)
	Middle		447 ± 118.9 (265-776)	199.6 ± 76.5 (85-370)	106.5 ± 56.4 (25-220)	41.7 ± 34.6 (0-115)	23.7 ± 21.2 (0-70)	17.8 ± 18.3 (0-65)	11.3 ± 13.3 (0-50)	5.3 ± 5.6 (0-19)	5.6 ± 4.6 (0-13)	0.6 ± 0.7 (0-2)	0.05 ± 0.22 (0-1)	25.9 ± 0.8 (24.8-27.6)	97.6 ± 3.7 (87.3-100)
	Far		344.4 ± 116.1 (185-711)	160 ± 67.5 (65-390)	87 ± 52.5 (30-270)	33.9 ± 29.2 (5-22)	16.6 ± 15.8 (0-70)	12.7 ± 14.5 (0-65)	7.3 ± 8.3 (0-35)	3.1 ± 3.9 (0-17)	3.0 ± 3.4 (0-14)	0.5 ± 1.1 (0-4)	0.04 ± 0.19 (0-1)	24.5 ± 0.6 (23.9-26.7)	90.7 ± 6 (80.4-100)
5	Near face	Mouth	439.7 ± 170.9 (240-851)	206.4 ± 98.6 (105-430)	107.7 ± 66.7 (45-250)	47.5 ± 32.7 (10-105)	20.2 ± 15.6 (0-55)	14.0 ± 11.7 (0-40)	7.1 ± 7.4 (0-20)	3.82 ± 03.7 (0-16)	3.32 ± 03.47 (0-11)	0.23 ± 0.43 (0-1)	0.0 ± 0.0 (0-0)	26.6 ± 0.8 (25.2-27.9)	93.2 ± 6.7 (80.5-100)
	Middle		509± 123.9 (265-736)	252 ± 84.5 (105-410)	136.3 ± 53.5 (50-255)	55.2 ± 23.8 (20-105)	27.9 ± 19.6 (0-75)	19.3 ± 16.8 (0-60)	11.1 ± 12.1 (0-40)	6.3 ± 5.9 (0-19)	5.1 ± 5.8 (0-15)	0.6 ± 0.7 (0-2)	0.03 ± 0.17 (0-1)	23.9 ± 0.4 (23-24.3)	86.9 ± 6.4 (75.3-97.9)
	Far		566 ± 103 (310-736)	303 ± 69.9 (125-375)	180 ± 46.7 (75-270)	125- ± 26.2 (20-125)	33 ± 15.2 (5-55)	25 ± 12.9 (5-45)	12.3 ± 7.7 (0-25)	4.6 ± 3.3 (0-12)	4.4 ± 3.2 (0-10)	0.5 ± 1.3 (0-5)	0.28 ± 1.1 (0-5)	24.5 ± 0.7 (23-26.6)	98.7 ± 2 (93.6-100)
	Near face	Nose	541 ± 166 (275-821)	256.1 ± 116.7 (55-475)	150.6 ± 81 (30-315)	69.3 ± 50.8 (5-170)	40.0 ± 31.7 (5-115)	31.6 ± 26.1 (0-90)	22.3 ± 19.8 (0-65)	11.9 ± 9.6 (0-36)	9.9 ± 9.4 (0-26)	1.9 ± 1.5 (0-5)	0.13 ± 0.40 (0-3)	24.6 ± 1 (22.5-25.7)	99.7 ± 1.1 (95.4-100)
	Middle		540 ± 125.5 (365-746)	265 ± 94.7 (130-445)	144.5 ± 67.8 (45-305)	65.9 ± 42.4 (10-165)	34.5 ± 27.4 (5-115)	25.7 ± 22.7 (0-85)	13.6 ± 16.3 (0-65)	12.82 ± 9.7 (0-36)	7.9 ± 8 (0-28)	1.6 ± 1.9 (0-7)	0.60 ± 1.2 (0-5)	24.4 ± 0.4 (23.7-24.8)	91.6 ± 5.9 (79.5-100)
	Far		433 ± 84.9 (320-635)	215 ± 77.7 (125-390)	109 ± 47.6 (225-55)	41.9 ± 24.7 (10-100)	17.6 ± 11.9 (0-40)	10.2 ± 8 (0-25)	3.9 ± 5.6 (0-20)	1.8 ± 2.7 (0-11)	1.7 ± 2.5 (0-7)	0.4 ± 0.6 (0-2)	0.03 ± 0.27 (0-2)	21.9 ± 0.9 (20.2-23)	97 ± 2.6 (91.5-100)
6	Near face	Combine	546.6 ± 146.3 (315-756)	294.3 ± 96.1 (150-435)	155.3 ± 71.1 (54-255)	63.5 ± 47 (16-170)	32.5 ± 34.3 (0-115)	31.3 ± 30.1 (0-102)	19.3 ± 21.8 (0-75)	8.6 ± 6.8 (0-22)	7.6 ± 6.6 (0-17)	1.2 ± 1.2 (0-4)	0.04 ± 0.19 (0-1)	25.5 ± 1.1 (23.3-27)	88.2 ± 6.8 (76.4-98.9)
	Middle		535.6 ± 86.8 (395-701)	269.6 ± 56.5 (185-355)	169.1 ± 48.2 (70-245)	79.3 ± 32.8 (25-125)	52.4 ± 25.9 (15-95)	43.4 ± 22.3 (15-90)	28.7 ± 18.4 (5-70)	22.4 ± 15.7 (5-50)	15.3 ± 7.5 (5-28)	2.4 ± 1.8 (0-7)	0.03 ± 0.16 (0-1)	26.6 ± 1.2 (24-28.2)	91.5 ± 7.9 (73.7-100)
	Far		339.7 ± 110.3 (205-625)	170.5 ± 57.6 (90-300)	92.1 ± 32.7 (50-165)	43.4 ± 22.3 (15-90)	28.7 ± 18.4 (5-70)	22.4 ± 15.7 (5-50)	13.4 ± 12.7 (0-45)	6.8 ± 5.3 (0-23)	4.9 ± 5.7 (0-17)	0.9 ± 1.2 (0-5)	0.0 ± 0.0 (0-0)	25.6 ± 1 (23.6-26.8)	87.7 ± 6.4 (74.8-96.3)
7	Near face	Mouth	352.5 ± 51.6 (260-455)	131 ± 41.1 (48-210)	62.3 ± 25.0 (22-108)	17.2 ± 12.8 (0-51)	6.7 ± 7.2 (0-32)	3.4 ± 5.7 (0-24)	0.9 ± 1.8 (0-7)	0.5 ± 1.4 (0-6)	0.4 ± 1.2 (0-5)	0.2 ± 0.4 (0-2)	0.09 ± 0.31 (0-2)	27 ± 0.9 (25.9-27.9)	93.3 ± 6.2 (79.1-100)

	Middle		402.1 ± 83.5 (265-545)	178.5 ± 70.8 (79-335)	98 ± 46.7 (48-195)	32.2 ± 21.6 (0-85)	19.1 ± 14.3 (0-48)	16.9 ± 15.2 (0-45)	8.5 ± 9.8 (0-30)	4.4 ± 4.8 (0-20)	3.7 ± 3.3 (0-13)	0.4 ± 1.1 (0-5)	0.06 ± 0.28 (0-2)	27.9 ± 0.6 (27.2-28.5)	83.4 ± 6.8 (71.8-92.8)
	Far		389.2 ± 132.7 (217-691)	162.9 ± 72 (69-400)	89.6 ± 59.3 (10-225)	32.2 ± 26.6 (0-89)	16.9 ± 19.2 (0-49)	13 ± 14.8 (0-39)	9.5 ± 9.8 (0-32)	4.4 ± 4.8 (0-21)	4 ± 4.9 (0-19)	0.4 ± 1.1 (0-5)	0.0 ± 0.0 (0-0)	26.7 ± 0.3 (26.2-27.2)	88.1 ± 6.4 (76.8-99.8)
	Near face	Nose	402.8 ± 83.5 (265-555)	188.5 ± 70.8 (70-335)	98 ± 46.8 (30-195)	61.5 ± 28.9 (20-79)	16.9 ± 15 (0-60)	12.8 ± 13.0 (0-51)	6.1 ± 7.5 (0-31)	3.1 ± 4.4 (0-21)	2.1 ± 3.6 (0-10)	0.7 ± 1.4 (0-6)	0.05 ± 0.21 (0-1)	26.6 ± 0.9 (24.7-27.9)	94 ± 6 (81.5-100)
	Middle		477 ± 118.1 (269-786)	199.1 ± 76.3 (89-379)	101.5 ± 53.4 (22-210)	41.1 ± 34.1 (0-125)	23.1 ± 21.2 (0-68)	17.1 ± 17.3 (0-55)	11.1 ± 11.3 (0-41)	5.1 ± 5.9 (0-19)	5.3 ± 4.4 (0-13)	0.6 ± 0.7 (0-2)	0.04 ± 0.19 (0-1)	25.9 ± 0.8 (24.8-27.6)	97.6 ± 3.7 (87.3-100)
	Far		324.4 ± 106.1 (175-701)	161 ± 65.5 (55-390)	87 ± 51.5 (30-259)	33.9 ± 29.2 (5-21)	16.6 ± 15.8 (0-64)	12.3 ± 14.1 (0-61)	7.3 ± 7.3 (0-39)	3.1 ± 3.8 (0-16)	3.0 ± 3.2 (0-14)	0.4 ± 1.1 (0-4)	0.08 ± 0.34 (0-2)	24.9 ± 0.7 (23.9-26.9)	90.7 ± 6 (82.4-100)
8	Near face	Combine	442.5 ± 62.1 (289-515)	252.5 ± 82.3 (155-385)	123 ± 34.4 (59-170)	51 ± 18.5 (15-80)	17.8 ± 9.4 (5-35)	9.3 ± 6.8 (0-25)	3.7 ± 4.2 (0-14)	2.4 ± 1.8 (0-11)	1.4 ± 1.6 (0-5)	0.6 ± 1.3 (0-4)	0.0 ± 0.0 (0-0)	24.1 ± 1.1 (22.7-26.8)	94.1 ± 3.9 (81.5-100)
	Middle		229.5 ± 49.1 (121-301)	95.5 ± 27.1 (39-145)	51 ± 17.5 (15-80)	17.3 ± 11.9 (0-50)	9.3 ± 6.8 (0-25)	17.3 ± 11.9 (0-50)	3.4 ± 3.7 (0-15)	1.8 ± 2.2 (0-8)	1.5 ± 2.1 (0-6)	0.7 ± 1.1 (0-3)	0.0 ± 0.0 (0-0)	22.7 ± 0.8 (21.8-23.8)	99.4 ± 0.7 (95.8-100)
	Far		212.8 ± 52.3 (90-315)	80.8 ± 34.3 (21-141)	33.3 ± 14.6 (5-84)	17.3 ± 11.2 (0-48)	12.7 ± 9.9 (0-40)	7.7 ± 8.7 (0-32)	17.5 ± 10.9 (0-51)	3.6 ± 3.9 (0-16)	3.2 ± 3.7 (0-13)	0.4 ± 0.7 (0-3)	0.11 ± 0.37 (0-2)	21.9 ± 0.8 (19.9-22.9)	99.9 ± 0.4 (98.9-100)
9	Near face	Combine	596.2 ± 166.9 (389-851)	299.3 ± 121.1 (179-475)	161.3 ± 80.1 (53-275)	63.5 ± 51 (15-150)	42.5 ± 18.0 (15-70)	31.3 ± 31.1 (0-102)	22.4 ± 15.7 (5-50)	9.3 ± 6.8 (0-25)	8.5 ± 7 (0-20)	1.3 ± 1.2 (0-4)	0.0 ± 0.0 (0-0)	25.9 ± 0.9 (23.9-27.9)	92.6 ± 3.7 (84.2-99.4)
	Middle		472.5 ± 82.1 (315-585)	272.5 ± 92.3 (165-485)	100.5 ± 29.1 (45-155)	75.3 ± 31.8 (23-121)	51 ± 18.5 (15-80)	42.5 ± 18.0 (15-70)	26.1 ± 16.3 (5-61)	17.3 ± 11.9 (0-50)	17.8 ± 9.4 (5-35)	2.3 ± 1.7 (0-7)	0.04 ± 0.19 (0-1)	24 ± 0.9 (22.9-24.9)	96.5 ± 3.4 (89.9-100)
	Far		359.7 ± 119.3 (209-645)	179.5 ± 59.6 (96-310)	97.1 ± 38.7 (53-175)	41.4 ± 21.3 (14-93)	29.7 ± 18.4 (5-72)	22.4 ± 16.7 (5-55)	12.5 ± 10.9 (0-40)	6.5 ± 7.6 (0-25)	3.4 ± 3.7 (0-15)	0.9 ± 1.3 (0-5)	0.01 ± 0.09 (0-1)	23.3 ± 1.2 (21-24.6)	98 ± 2.7 (92.9-100)
10	Near face	Combine	468.5 ± 82.1 (325-545)	279.9 ± 91.9 (159-465)	113 ± 38.4 (55-180)	42.5 ± 18.0 (15-70)	14.5 ± 8 (0-25)	8.5 ± 7 (0-20)	3.8 ± 3.9 (0-15)	2.4 ± 1.8 (0-12)	1.5 ± 2.2 (0-8)	0.6 ± 1.2 (0-4)	0.10 ± 0.37 (0-2)	24.5 ± 1.2 (21.3-27)	86.2 ± 6.8 (79.4-98.9)
	Middle		267.5 ± 49.1 (129-319)	93.5 ± 26.1 (49-145)	59 ± 16.5 (15-89)	17.3 ± 11.9 (0-50)	9.3 ± 6.8 (0-25)	6.5 ± 7.6 (0-25)	3.4 ± 3.7 (0-15)	1.7 ± 2.1 (0-10)	1.4 ± 2.1 (0-8)	0.7 ± 1 (0-3)	0.05 ± 0.21 (0-1)	25.6 ± 1.3 (23.1-27.2)	90.5 ± 7.2 (73.7-100)
	Far		238.8 ± 72.3 (90-321)	93.8 ± 31.4 (20-145)	39.1 ± 15.6 (5-76)	17.3 ± 11.6 (0-50)	11.5 ± 10.9 (0-40)	7.5 ± 8.5 (0-30)	6.5 ± 7.6 (0-25)	3.4 ± 3.9 (0-13)	3.1 ± 3.5 (0-14)	0.4 ± 0.9 (0-3)	0.05 ± 0.22 (0-1)	24.7 ± 1.1 (22.5-26.1)	85.7 ± 6.1 (81.8-96.3)

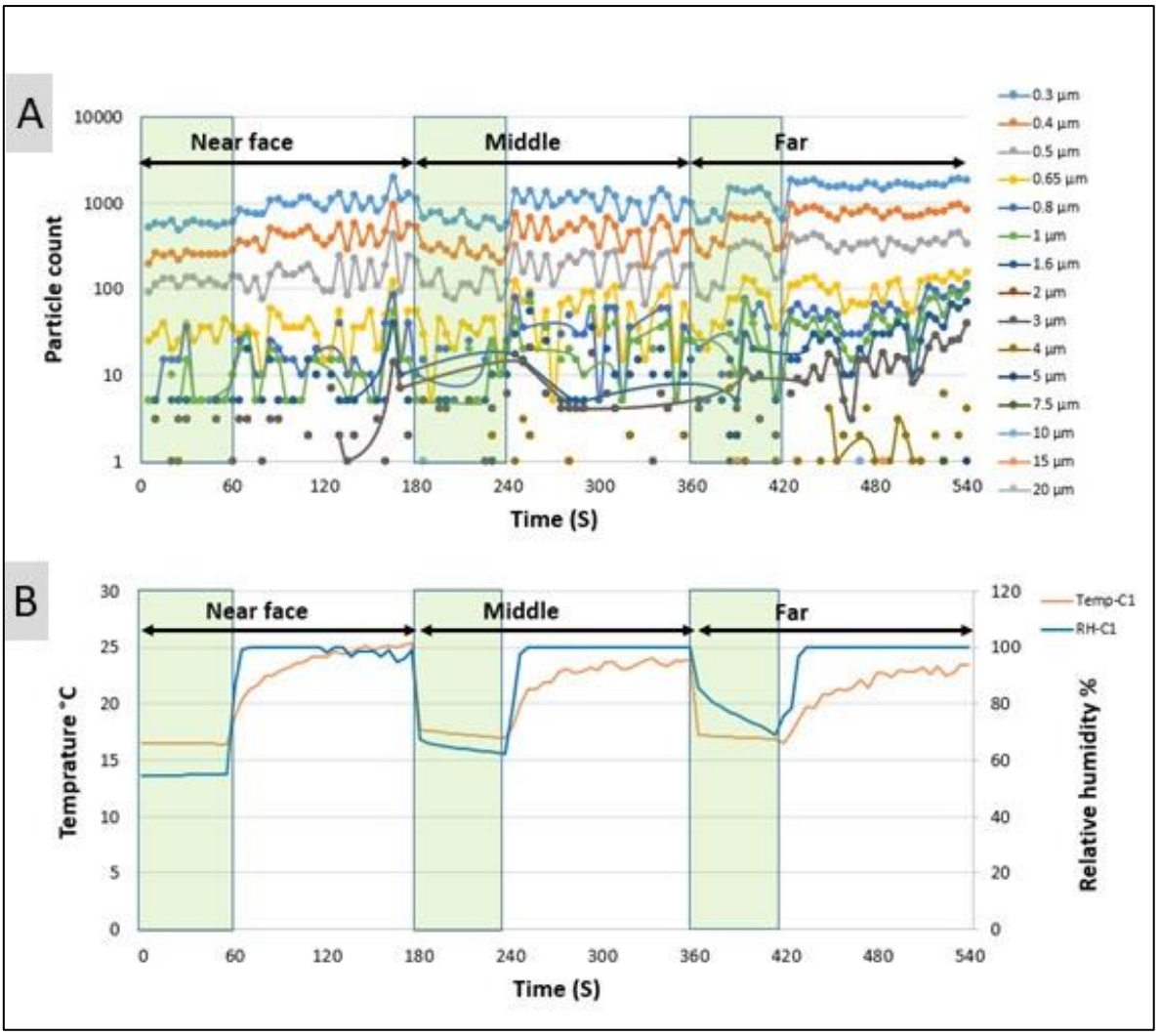

Figure 2: Measurement of the temporal changes from a single participant of A) size distribution of exhaled aerosols and droplets, and B) temperature and relative humidity in the three measurement points. The coloured boxes mark periods when the background environmental conditions were measured prior to sampling from the mask. Note the rapid equilibration of in facemask relative humidity (blue line) and slower equilibration of temperature (red line).

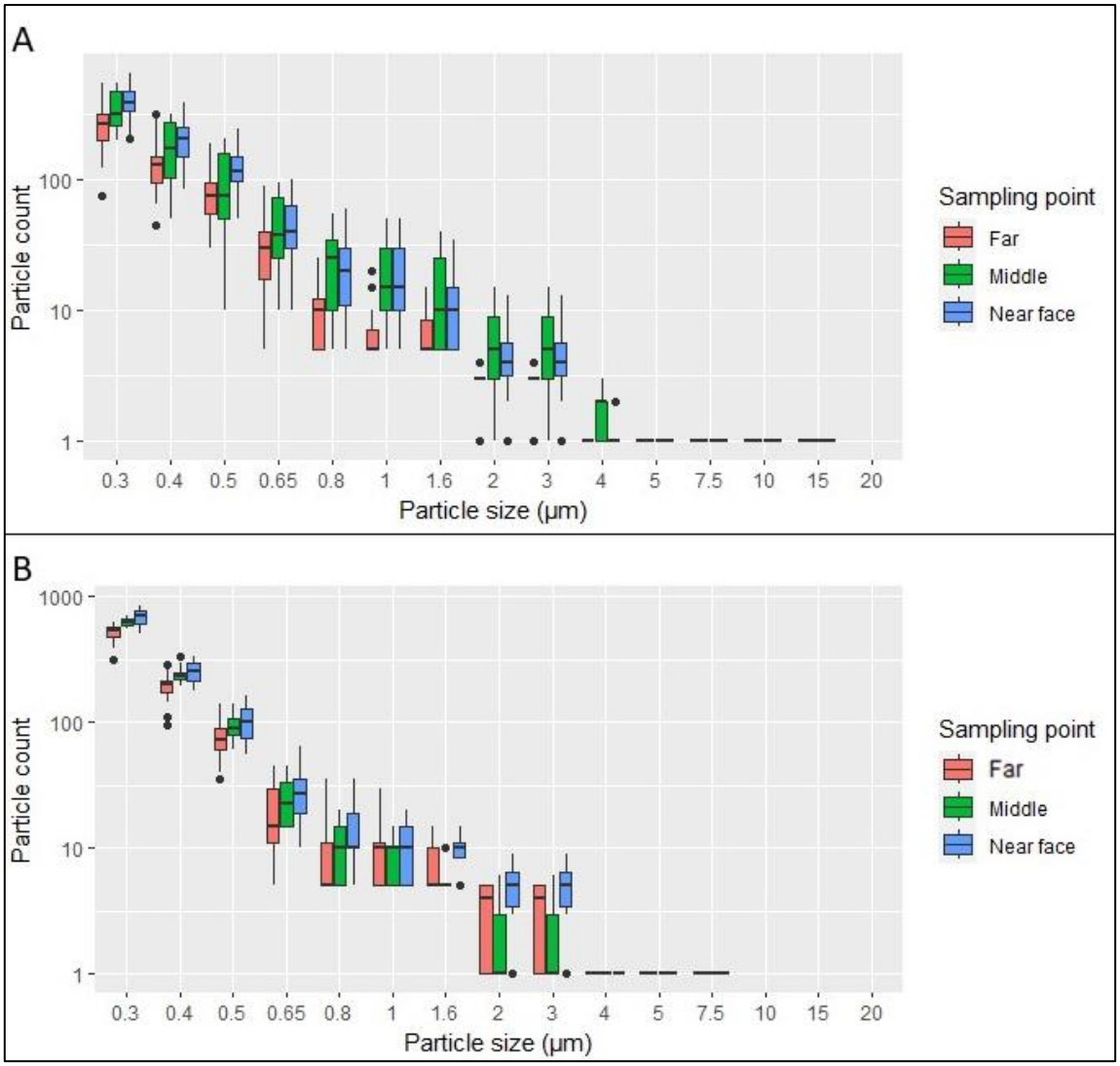

Figure 3a: Plots of particle counts for different particle size classes in the near, middle, and far chambers with a logarithmic count scale. A) Results from participant number 6 (combined breathing), and B) participant number 9 (combined breathing). The overall trends are similar, with decreasing counts from near to far chambers in most particle size classes, but there are marked differences in the particle size distribution produced by each participant.

The results show an expected decrease in particle count sizes from the near, through middle, to far locations. Larger sizes are too low in number (<10) to be statistically significant. However, a marked change in the particle counts with distance in the facemask is noted in several participants from 0.65 to 1 µm (typically 20-40%), which shows that the facemask design can be effective in segregating these populations.

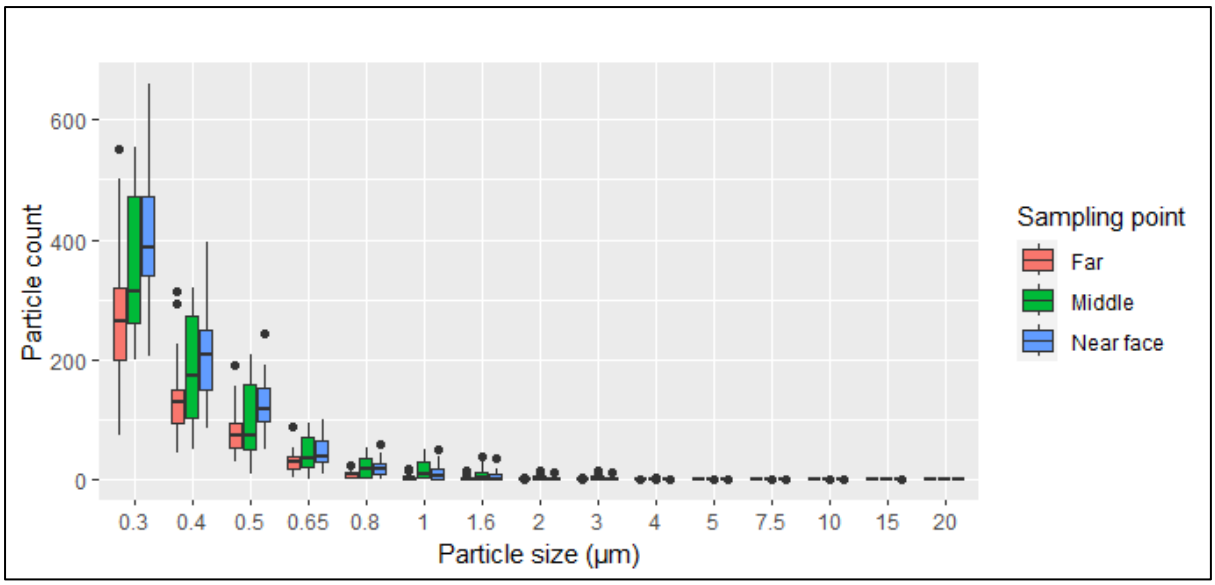

Figure 4b: Plot of particle counts for different particle size classes in the near, middle, and far chambers with a linear count scale for participant 6.

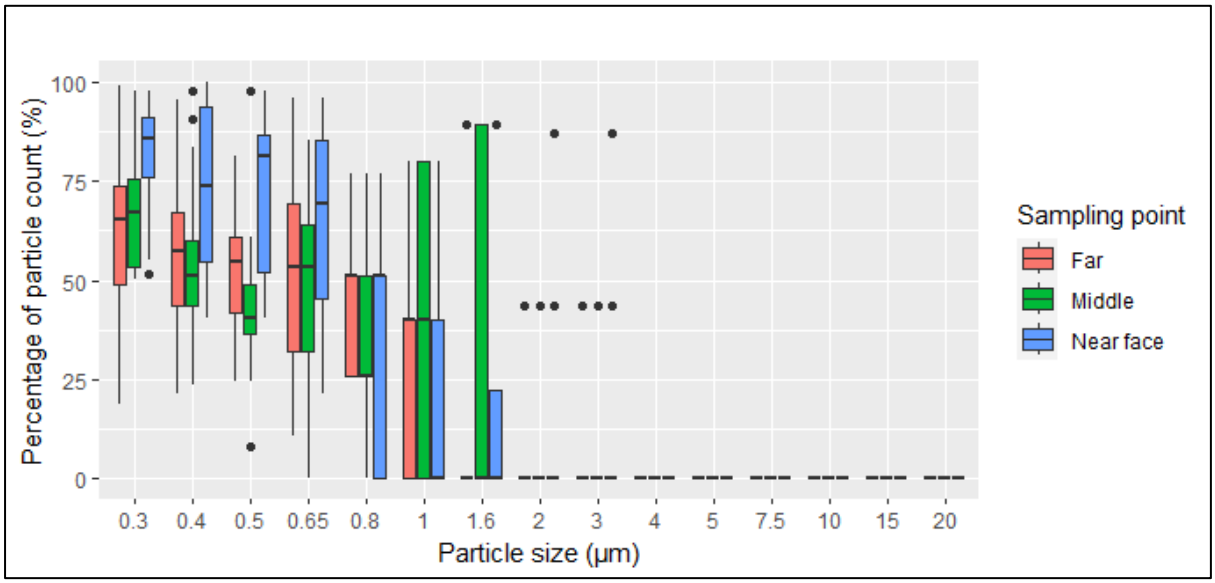

Figure 5c: Plot of percentage for different particle size classes in the near, middle, and far chambers with a linear count scale for participant 6. Note the significant decrease in the far chamber from 0.65-1 µm range.

Comparison of Mouth and Nose Breathing

There were four participants, participants 3, 4, 5, and 7, who performed nose-only, and mouth-only breathing during the experiments in order to investigate differences in particle size generation, and to support future development of the most appropriate measurement and monitoring protocols (**Table 1**). **Figure 6** shows a distinct difference between mouth and nose breathing in the aggregate of the four participants. Overall, nose breathing results in high particle counts in the middle chamber for all size classes, and mouth breathing results in higher particle counts in the far chamber for all

particle size classes. In some humans, nose breathing causes a 7.5-20 µm particle size to appear in the middle chamber (**Figure 6-A**). While the same size comes from the mouth breathing of other humans, it is detected only in the far chamber (**Figure 6-B**). These results suggest that differences in breathing type results in marked differences in primary particle size populations, and different fluid dynamic behaviour (I.e., velocity, pulses), which require further investigation. The impact of each participant's breathing type (combined, nose, and mouth) on the particle size population, the release dynamics, and subsequent segregation in the sampling facemask is inherently complicated, and background levels will need to be kept as low as possible before each test. However, a sampling protocols clearly need to consider breathing type.

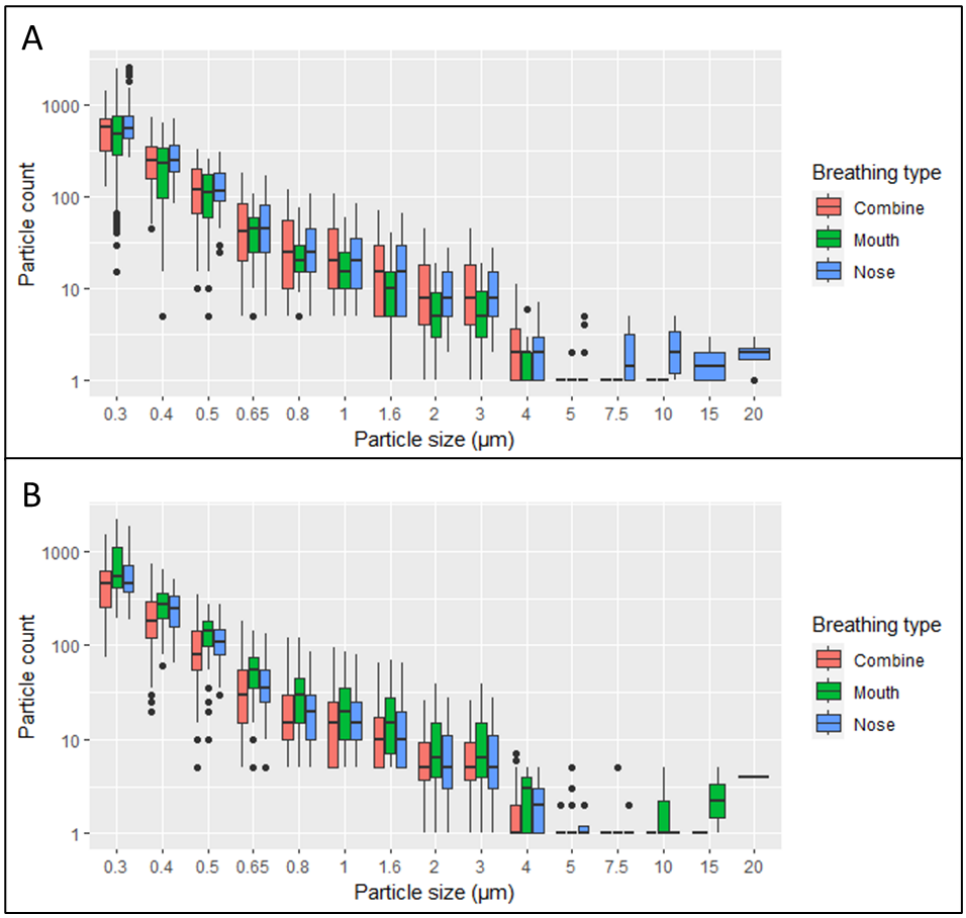

Figure 6 : The particle count for different particle size classes with different breathing styles. A) in the middle chamber and B) in the far chamber.

Water-sensitive paper strips

Syngenta water-sensitive paper strips were used to investigate the distribution of droplets within different mask chambers. The paper changes from yellow to dark blue in the presence of water, giving a rapid and highly visual indication of exhaled droplet locations, or condensed vapour as it cools from mouth outwards. **Figure 6** shows the results of water sensitive paper placed in the middle

(A) and far chambers (B) after one minute of combined breathing. In all participants, the facemask clearly segregates particle size as we see different amounts impacted in the different zones. The paper was placed in the mid-point and base of each chamber. For the same chamber and participant, the amount of colour change is higher on the base strip than in the middle strip.

The future utility of the water sensitive paper, and their improvement as a proxy for sampling strips, will need to establish both the suitable positions for sampling strips within this mask, and the appropriate experimental duration. A key benefit of this mask design is the nozzle component, which likely leads to optimal sampling regions that are relatively independent of face shape or mouth / nose breathing

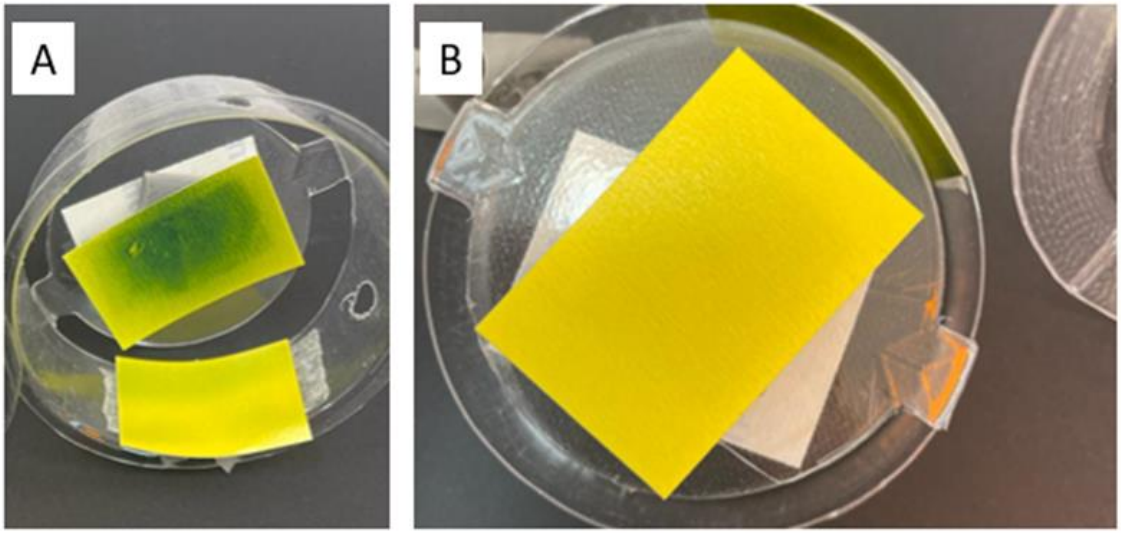

Figure 7: Syngenta water-sensitive paper strips A) in the middle chamber B) in the far chamber.

4.4 Thermal camera imagery

A FLIR A6750c medium wave infrared camera (MWIR) was used to capture images of a human subject wearing an early version of the facemask without the outer chambers. The camera was fitted with a narrow band filter that limited optical transmission to between 4100-4400 nm. Carbon dioxide (CO_2) has a series of optical adsorption bands between 4200 and 4300 nm, which means that MWIR cameras are highly sensitive to optical adsorption of CO_2 and allows visualization of CO_2 at room temperature (CO_2 conc > 1%). Prior to each subject the camera was calibrated using a black body radiation target. The mask was adjusted to fit the subject as well as possible. Each subject was recorded immediately after wearing the facemask for 180 seconds (at 25 Hz).

Figure 8 shows the comparison between two participants wearing an early version of the sampling facemask. The sequence of images for each participant represents a single evenly spaced exhalation

cycle. **Figure 8A** shows that participant **A** only exhibits a single exhalation plume from the end of the mask, likely the mask is a good fit. **Figure 8B** shows that participant **B** exhibits two exhalation plumes, one from the end of the mask and a second from the bridge of the nose, likely this is a result of a leak. This highlights a possible limitation with sampling masks as participant **B** would likely deposit less droplets of all sizes within a sampling mask as a consequence of the poor mask fit for their face type.

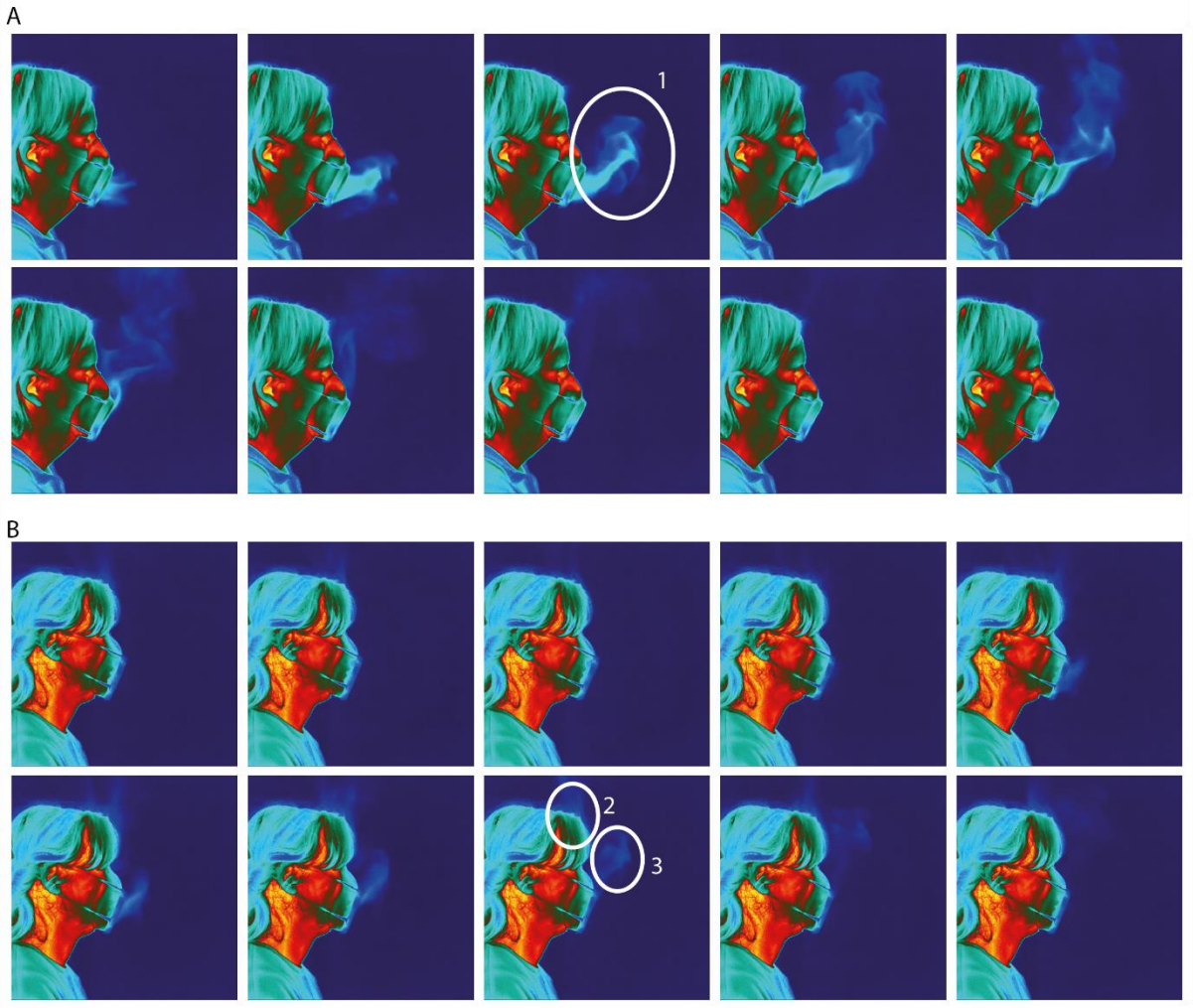

Figure 8: Comparison of two subjects wearing Leeds mask showing different fit characteristics. A. Participant A, illustrating only single plume during exhalation and likely a good fit. B. Participant B, illustrating two plumes, suggesting the presence of a leak at the bridge of noise.

Conclusion

Our study concludes that a bespoke sampling facemask has the potential to separate exhaled human breath particles by size. Our work shows promise from a pure fluid dynamics perspective but requires further work using human subjects to build on our core understanding. There is an inherent

complexity in considering multi interacting environmental parameters, and the natural variability of human face physiography and respiratory physiology. Nonetheless, for the first time we have documented and analysed important trends that tantalisingly point to the future use of sampling facemasks during disease outbreaks.

The key findings of this research include (i) that the particle count fluctuates with exhaling and inhaling, as shown clearly in the results after a minute of wearing a mask and breathing into it; (ii) the temperature and relative humidity reach steady states in each chamber after 20 seconds, suggesting that the sampling duration can be shortened; (iii) the sampling facemask shows a clear segregation to complete elimination, in particles sizes larger than 5 µm in most participants irrespective of breathing style; (iv) the evidence for size segregation and particle count is supported by placing water-sensitive paper in the mask, which shows a clear change of colour in the middle chamber no change of colour in the far chamber; (iv) mouth and nose breathing using the facemask demonstrate distinct differences in the particle count of different particle sizes in middle and far chamber, and these differences depend on the individual person wearing the mask, which points to a need to establish repeatable protocols when using the sampling facemasks.

Future work

The Covid-19 pandemic has vividly highlighted that better informed and earlier interventions can minimise transmissions, and limit socio-economic impacts. A bespoke sampling facemask is one instruments that could offer support in early intervention and monitoring. The dynamic environmental conditions, the natural variability between human subjects in particle generation and breathing fluid dynamics, establishes an inherently complicated system to analyse. The complexity of natural breathing dynamics, and variability between subjects, is likely due, in part, to variations in velocity during a breathing cycle. This is supported by observations of good size segregation with a constant flow mannequin head in earlier phases of work. Larger chambers (near the face), with samplers inside, would likely even these variations.

Whilst for the first time we have established experimental and analytical methods to document segration of size between a wide range of subject, this field of research requires further investigation to improve the understanding of particle emission dynamics, and to account for individual human factors (face shape, respiratory dynamics) by studying a larger number of participants. Other factors that must be considered in the research include (i) lowering the particle count of the background to reduce the effect of noise in the controlled environment to establish absolute differences; (ii) measuring the particle count in all chambers simultaneously; (iii) document the particle counts for the same participant using all breathing settings (mouth, nose, and combined), and over different

durations (1 minute, 2 minutes, etc.); and (iv) integrate the sampling strips to test and validate the virus types and load.

References

Milton, D.K., 2020. A Rosetta Stone for understanding infectious drops and aerosols. Journal of the Pediatric Infectious Diseases Society, 9(4), pp.413-415.

QUANTIFOIL Instruments GmbH Q.Instruments. Water-sensitive paper for monitoring spray distribution, 2008.

Wang, C.C., Prather, K.A., Sznitman, J., Jimenez, J.L., Lakdawala, S.S., Tufekci, Z. and Marr, L.C., 2021. Airborne transmission of respiratory viruses. Science, 373(6558), p.eabd9149.

Williams, C. et al., 2020. Exhaled Mycobacterium tuberculosis output and detection of subclinical disease by face-mask sampling: prospective observational studies. *The Lancet Infectious Diseases,* 20(5), pp. 607-617.

Williams, C. et al., 2014. Face mask sampling for the detection of Mycobacterium tuberculosis in expelled aerosols. *PloS one,* 9(8), p. e104921.